SR-MPC via LMIs Approach Applied to 3SSC Boost Converter Voltage Control

Roberta R. T. Alves * **Luís Carvalho** * **Marcus V. S. Costa** *
Francisco E. U. Reis **

* *Universidade Federal Rural do Semi-Árido, RN, (e-mail: robertarafaela2010@hotmail.com, luiscarvalho9000@gmail.com, marcus.costa@ufersa.edu.br)*
** *Universidade Federal do Piauí, PI, (e-mail: evertonsx@gmail.com)*

Abstract:
This paper proposes the application of a switched robust predictive control applied to output voltage control of a three-state switching cell boost converter considering the average space-state equivalent boost model. The proposed technique follows the switched quadratic performance index minimization principle modeled via linear matrix inequalities (LMIs) to closed-loop stabilization problem of a boost converter. The simulation results evidence the closed-loop stabilization of the presented converter using the switched predictive control demonstrated through the time response analysis and the closed-loop boundary ellipsoids procedure. This study demonstrated that the proposed control technique is suitable to output voltage control of boost converter. As future works are the validation test in the experimental setup.

Keywords: Model Predictive Control; Linear Matrix Inequalities; Switched Systems; Boost Converter CCTE; robust stability.

1. INTRODUCTION

Studies involving the Robust Model Predictive Control (RMPC) applications via linear matrix inequalities (LMIs) to power electronics converters have been worth of investigation accord to Costa et al. (2016, 2017) and Rego et al. (2018). Moreover, the RMPC-LMI design techniques demonstrate its efficacy to output voltage control of the boost converters as seen in Rego et al. (2019); Rego and Costa (2019); Moreira et al. (2019) and Araújo et al. (2019)).

The main advantage of the boost converter classic modeling is its capability to perform original topology of DC-DC and AC-DC boost converter through the boost equivalent model (Middlebrook and Cuk, 1976). However, the existence of the non-minimum phase, associated with the parameters variations such as load and input voltage difficulty the closed-loop stabilization for only one point operation design control (Bascopé and Barbi, 2000; Costa et al., 2017).

Besides, solutions for robust predictive control design are presented by Moreira et al. (2019, 2021), in which proposed a Generalized Predictive Control and constrained RMPC-LMI with fuzzy approach respectively. Thus, the features of RMPC-LMI design are usually applied to constrained multivariable models with uncertainty processing as seen in Peccin et al. (2019); Cao et al. (2021); Fard and Sadeghzadeh (2021) and Kaitao et al. (2022).

Furthermore, the power converters structure design use the switching principle aiming to energy conservation (Bascopé and Barbi, 2000). Though, the switching approach used in power electronics are nonlinear, where its linearization follows the average state space approach or PWM method Costa et al. (2017). As alternative capable to solve the closed-loop switching problem is the switching design control as presented in Dey et al. (2021); Kairuz et al. (2021) and Najson (2021), where presented solutions to switched systems as existent in power converters.

For example, Hall and Bridgeman (2021) and Marcolino et al. (2020) proposed model predictive control techniques for switched linear systems. Hall and Bridgeman (2021) developed a study about exogenous switching in predictive control. Marcolino et al. (2020) discussed a switched predictive control application involving two or more control laws through linearized systems in function of structured uncertainties.

Moreover, are highlighted the works of Benallouch et al. (2014); Maestre et al. (2010); Khan et al. (2020). The first article developed a LMI procedure to solve a switched predictive control design problem. Maestre et al. (2010) proposed an adaptive predictive controller using multiple linear subsystems which the local control laws are scaled in an algorithm where the global control law is determined by a switching rule. Finally, Khan et al. (2020) applied a switched predictive control methodology in a novel power inverter used to photovoltaic grid connected system.

Following the aforementioned background, this paper proposes a switched robust model predictive control (SR-MPC) applied to boost converter output voltage control. The proposed design uses the approach of Kothare et al. (1996) and follows the switched model predictive control procedure of Benallouch et al. (2014) using LMIs, which aims to minimize the upper quadratic performance index considering an infinite horizon prediction.

Besides, the contribution of this study is the follows: (i) A synthesis control design of a Switched RMPC-MLMI to the boost converter using average state-space model; (ii) a switched closed-loop stability analysis considering a switched polytopic uncertainty approach, testing the algorithm to more complex conditions than the study of Benallouch et al. (2014); (iii) a simulation testing of the SR-MPC-LMI in the 3SSC boost converter used by Rego et al. (2019); Rego and Costa (2019); Moreira et al. (2019) and Moreira et al. (2021), adopting the variation parameters based the switching principle of Geromel and Colaneri (2006a); Benallouch et al. (2014).

This paper is divided as follows: The Section 2 presents the 3SSC converter and explains the average state-space modeling used in this study. The Section 3 shows the proposed control design using switched principle approach. In Section 4, the simulation results are illustrated, analyzed and discussed. Finally, the Section 5 summarizes the findings found in this study and proposes future works.

2. CONVERTER MODELING

The Three State Switching Cell (3SSC) Boost Converter circuit proposed by Costa et al. (2017) is illustrated in Figure 1. Besides, the Table 1 displays the parameters the converter used in this study (Costa et al., 2017).

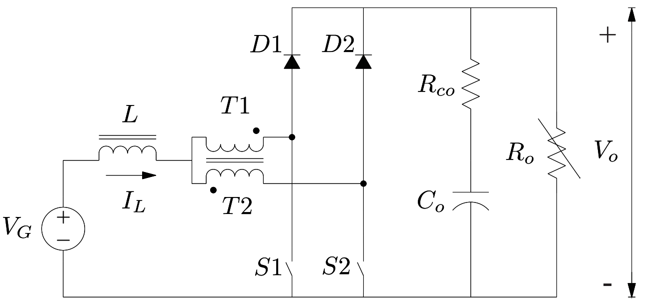

Figura 1. 3SSC Boost Conveter (Costa et al., 2017).

Tabela 1. Boost Converter Parameters.

Parameters	Values
Input Voltage (V_G)	$26 - 36$ $[V]$
Output Voltage (V_o)	48 $[V]$
Frequency (f_s)	22 $[kHz]$
Inductor (L)	36 $[\mu H]$
Inductor Resistor (R_L)	0 $[\Omega]$
Capacitance (C_o)	4.400 $[\mu F]$
Capacitor equivalent resistor (R_{co})	$26,7$ $[\mu\Omega]$
Load (R_o)	$2,034 - 6,06$ $[\Omega]$
Output Power	$380 - 1.000$ $[W]$
Sample Time	1 $[ms]$

The 3SSC boost converter model is reduced to average state-space model matrices A, B, C and D, considering the Continuous Driving Mode (CDM) (Middlebrook and Cuk, 1976; Rego et al., 2018) defined by:

$$\begin{aligned} x(k+1) &= Ax(k) + Bu(k) \\ y(k) &= Cx(k) + Du(k) \end{aligned} \tag{1}$$

where,

$$A = \begin{bmatrix} -\frac{R_L+(1-D_{cycle})(R_{co}\|R_o)}{L} & -\frac{(1-D_{cycle})R_o}{L(R_{co}+R_o)} \\ \frac{(1-D_{cycle})R_o}{C_o(R_{co}+R_o)} & -\frac{1}{C_o(R_{co}+R_o)} \end{bmatrix} \tag{2}$$

$$B = \begin{bmatrix} \frac{R_{co}}{L}\frac{(1-D_{cycle})R_o+R_{co}}{(R_{co}+R_o)} \\ -\frac{R_o}{C_o(R_{co}+R_o)} \end{bmatrix} \tag{3}$$

$$C = \begin{bmatrix} (1-D_{cycle})(R_{co} \parallel R_o) \frac{R_o}{(R_{co}+R_o)} \end{bmatrix} \tag{4}$$

$$D = -V_g \frac{R_{co} \parallel R_o}{R'} \tag{5}$$

Where $R' = (1-D_{cycle})^2 R_o + D_{cycle}(1-D_{cycle})(R_{co}\|R_o)$. The state variable $x = [i_L \ \ v_c]^T$ are the inductor current (i_L) and the capacitor voltage (V_c) respectively. D_{cycle} is the duty cycle, u is the control signal and y is the output voltage (V_o).

3. CONTROL STRATEGY

The switched linear systems theory is divided in two groups. The first group, the switching rule $\sigma(\cdot)$ not depends of states equivalent to time variant uncertainty. The second group, $\sigma(\cdot)$ is a control variable that depends of state or of system. Both groups, the main objective is to obtain a switching rule $\sigma(\cdot)$ that assures the global asymptotic stability system (Deaecto and Geromel, 2008). Considering this context, follows

$$x(k+1) = A_{\sigma(k)}x(k), \ x(0) = x_0. \tag{6}$$

For all $k \geq 0$, $x(k) \in \mathbb{R}^n$ is the available state to feedback, $\sigma(k)$ is the switching rule and $x_0 \ \epsilon \ \mathbb{R}^n$ is the initial condition. Hence, to each sample time, the switching rule chooses $A_{\sigma(k)} \ \epsilon \ \mathbb{R}^{n\times n}$ of set $\{A_1, \ A_2, \ A_3, \ldots, A_N\}$. The global asymptotic stability conditions are achieved through the Lyapunov functions, given by:

$$v(x) = \min_{i\epsilon\mathbb{K}} \ x' \ P_i x = \min_{\lambda\epsilon\Lambda} \left(\sum_{i=1}^{N} \lambda_i x' P_i x \right), \tag{7}$$

where, $P_i, \forall i \in \mathbb{K}$ are positive-defined symmetric matrices and $\lambda \in \mathbb{R}^N$ is a variable of the convex hull Λ, defined by

$$\Lambda = \left\{ \lambda \in \mathbb{R}^N : \sum_{i=1}^{N} \lambda_i = 1, \ \lambda_i \geq 0 \right\}. \tag{8}$$

To enhance the comprehension, let $I(x) = i \in \mathbb{K} : v(x) = x' P_i x \subset \mathbb{K}$ is the indices set. To situations that the minimization condition defined in (7) is not unique, the set $I(x)$ has more than one element (Deaecto and Geromel, 2008). Thence, the idea is to achieve a switching rule $g(x) : \mathbb{R}^n \to \mathbb{K}$ and conditions to $\sigma(k) = g(x(k))$ operates that (6) can be a global point. Thence, it is adopted the Theorem of Geromel and Colaneri (2006b) that satisfies the closed-loop stabilization conditions to switched linear systems.

ISSN: 2525-8311

DOI: 10.20906/CBA2022/3388

3.1 SR-MPC approach

Based in Benallouch et al. (2014) and Esfahani and Pieper (2019), consider the switched linear system given by (9).

$$\begin{aligned} x(k+1) &= A_{\sigma(k)}x(k) + B_{\sigma(k)}u(k) + W_{\sigma(k)}w(k) \\ z(k) &= C_{\sigma(k)}x(k) + D_{\sigma(k)}u(k) \end{aligned} \tag{9}$$

In (9) system, $x(k) \in \mathbb{R}^n$ are the states of system, $u(k) \in \mathbb{R}^m$ is the control signal, and $z(k) \in \mathbb{R}^q$ is the output signal, and $w(k) \in \mathbb{R}^r$ is the exogenous disturbance system, defined in (10).

The matrices $A_{\sigma(k)}$, $B_{\sigma(k)}$, $W_{\sigma(k)}$, $C_{\sigma(k)}$, $D_{\sigma(k)}$ are state matrix, input matrix, disturbance matrix, output matrix, and transmittance matrix respectively. All the aforementioned matrices follow the switching rule for each sample time, where the presented matrices contain N subsystems that are clustered in the global model, subjected by switching method as displayed in (10) in (11).

$$\mathbb{W} = \left\{ w \in \mathbb{R}^r \;\middle|\; \left\|W\right\|_{\mathcal{L}_2^r} \leq w_{\max} \right\} \tag{10}$$

$$\sigma(k) \in \mathbb{N}, \quad \mathbb{N} = \{1,\ 2,\ 3,\ \ldots,\ N\}, \quad \forall \ \ k \geq 0 \tag{11}$$

Accord to Geromel and Colaneri (2006a), it assumed that the Lyapunov stability criteria to switched rule along with the comutation rule, given by (12) and (13), respectively.

$$V\left(x\left(k|k\right), \sigma\left(k\right)\ \right) = x\left(k|k\right)^T P_{\sigma}(k) x\left(k|k\right) \tag{12}$$

$$\sigma\left(x\left(k\right)\right) = \arg \min_{\sigma(k)\ =\ i\ \in\ \mathbb{N}} x\left(k|k\right)^T P_{\sigma(k)} x\left(k|k\right) \tag{13}$$

In (12) and (13), $P_{\sigma(k)}$ is the correspondent matrix for respective subsystem, in which $x(k_1|k_2)$ are the system states at instant k_1 predicted from of moment k_2.

Add to this, suppose the existence of constraints that limits the control signal and the states as well as described in (14) and (15), consequently.

$$\mathbb{U} = \left\{ u(k) : -u_{\lim}^{z_d} \leq u^{z_d}(k) \leq u_{\lim}^{z_d},\ z_d = 1,\ 2,\ 3,\ \ldots,\ m \right\} \tag{14}$$

$$\mathbb{X} = \left\{ x(k) : -x_{\lim}^{v_d} \leq x^{v_d}(k) \leq x_{\lim}^{v_d},\ v_d = 1,\ 2,\ 3,\ \ldots,\ n \right\} \tag{15}$$

To SR-MPC syntesis, the IH-based quadratic performance index proposed by Benallouch et al. (2014) is expressed in (16).

$$J_\infty\left(k\right) = \sum_{k=0}^{\infty} \left\|x\left(k\right)\right\|_{R_x}^2 + \left\|u\left(k\right)\right\|_{R_u}^2 - \lambda^2 \left\|w\left(k\right)\right\|_{R_w}^2 \tag{16}$$

Where (16), $\lambda > 0$ is the noise attenuation constant, $R_x = C_{\sigma(k)}^T C_{\sigma(k)} > 0$, $R_u = D_{\sigma(k)}^T D_{\sigma(k)} > 0$ and $R_w > 0$. To obtain the feedback state gain given by $F_{\sigma(k)} = Y_{\sigma(k)} G_{\sigma(k)}^{-1}$, to $G_{\sigma(k)} \geq 0$ and $S_{\sigma(k)} = S_{\sigma(k)}^T \geq 0$, it is necessary that (17) must be feasible.

$$\min_{S_\sigma,\ G_\sigma,\ X_\sigma} \eta \tag{17}$$

Subjected to:

$$\begin{bmatrix} G_i + G_i^T - S_i & * & * & * \\ A_iG_i + B_iX_i & S_j & * & * \\ C_iG_i + D_iX_i & 0 & \eta I & * \\ 0 & \eta W_i^T & 0 & \eta\mu R_w \end{bmatrix} \geq 0 \tag{18}$$

$$\begin{bmatrix} 1 & * & * \\ \mu w_{\max}^2 & \eta\mu w_{\max}^2 & * \\ x\left(0\right) & 0 & S_i \end{bmatrix} \geq 0 \tag{19}$$

$$\begin{bmatrix} Z_i & * \\ X_i & G_i + G_i^T - S_i \end{bmatrix} \geq 0 \tag{20}$$

$$\begin{bmatrix} V_i & * & * \\ A_iG_i + B_iX_i & \omega_{\max}^{-1}\left(G_i + G_i^T - S_i\right) & * \\ W_i & 0 & \omega_{\max}^{-1} I \end{bmatrix} \geq 0 \tag{21}$$

Where $Z_i \ \leq (u_{\lim}^{z_d})^2$ and $V_i \ \leq (x_{\lim}^{v_d})^2$ in which, $z_d = 1,\ 2,\ 3,\ \ldots,\ m$ e $v_d = 1,\ 2,\ 3,\ \ldots,\ n$. The disturbance is norm limited by $w_{\max}$ and $\omega_{\max} = 1 + w_{\max}^2$. The attenuation constant and performance index upper limit are given by $\lambda = \sqrt{\mu}$ e $\beta = \sqrt{\eta}$, respectively. Besides, the stability matrix of system follows the relaxation approach proposed by Cuzzola et al. (2002), being used to robustness analysis by boundary ellipsoids (Wan and Kothare, 2002; Kothare et al., 1996; Rego et al., 2018; Moreira et al., 2021). It also highlighted that the proposed optimizing procedure can be adjusted considering as objective function μ or η to avoid the bilinearity problem (Benallouch et al., 2014).

4. SIMULATION RESULTS

This section is divided in two parts. The first part explains the servomechanism of integral action used in Moreira et al. (2021) and Costa et al. (2017). The second part analyses and discusses the results obtained by simulation using the SR-MPC proposed in this study.

Besides, the numerical model is divided in two subsystems modeled from of load variation. Both the subsystems use two polytopes vertices, in which the switching rule follows the input voltage variation. The numerical example follows the study of Rego et al. (2019).

4.1 Servomechanism of Integral Action

The servomechanism of integral action block diagram used in this study along with the SR-RMPC procedure is illustrated in Fugure 2 (Costa et al., 2017). Thence, the expressions of augmented model used to servomechanism design are given by:

$$\begin{aligned} x(k+1) &= \bar{A}_{\sigma(k)}x(k) + \bar{B}_{\sigma(k)}u(k) \\ y(k) &= \bar{C}_{\sigma(k)}x(k) + \bar{D}_{\sigma(k)}u(k) \end{aligned} \tag{22}$$

in which,

$$\bar{A}_{\sigma(k)} = \begin{bmatrix} A_{\sigma(k)} & 0 \\ -hC_{\sigma(k)} & g \end{bmatrix}, \quad \bar{B}_{\sigma(k)} = \begin{bmatrix} B_{\sigma(k)} \\ -hD_{\sigma(k)} \end{bmatrix}, \tag{23}$$

$$\bar{C}_{\sigma(k)} = \begin{bmatrix} C_{\sigma(k)} & 0 \end{bmatrix}, \quad \bar{D}_{\sigma(k)} = \begin{bmatrix} D_{\sigma(k)} \\ 0 \end{bmatrix}. \tag{24}$$

The closed-loop model with the switched-gain $F_{\sigma(k)} = -[F_{\sigma(k)}^a \ \ - F_{\sigma(k)}^b]$ are expressed by:

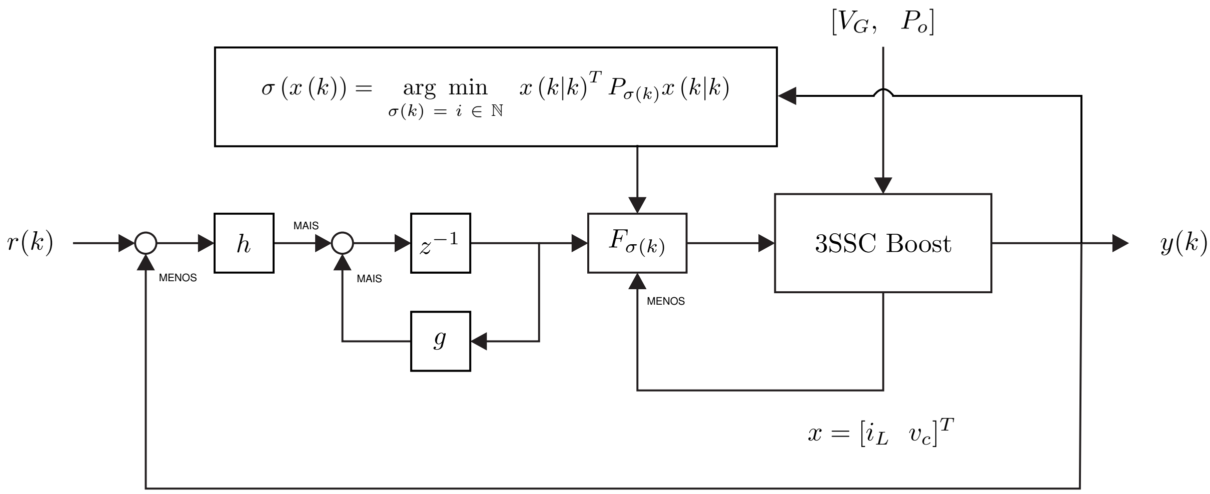

Figura 2. Proposed control design block diagram.

$$\begin{bmatrix} x(k+1) \\ v(k) \end{bmatrix} = \begin{bmatrix} A_{\sigma(k)} - B_{\sigma(k)} F^a_{\sigma(k)} & B_{\sigma(k)} - F^b_{\sigma(k)} \\ -h(C_{\sigma(k)} - D_{\sigma(k)} F_{\sigma(k)}) & g - hD_{\sigma(k)} F^b_{\sigma(k)} \end{bmatrix} \begin{bmatrix} x(k) \\ v(k) \end{bmatrix} + \begin{bmatrix} 0 \\ h \end{bmatrix} r(k), \tag{25}$$

$$y(k) = \begin{bmatrix} (C_{\sigma(k)} - D_{\sigma(k)} F_{\sigma(k)}) & D_{\sigma(k)} F^b_{\sigma(k)} \end{bmatrix} \begin{bmatrix} x(k) \\ v(k) \end{bmatrix} \tag{26}$$

where $(r(k))$ is the setpoint, $(v(k))$ is the integral action and (g) e (h) are the degree of freedom gains. These gains are used to fine tuning of closed-loop response model.

4.2 Analysis of results

The numerical model of boost converter are given by $-Subsystem - 1.1 - V(36V,\ 1000W)$

$$A_1 = \begin{bmatrix} -0.2838 & -7.7479 \\ 0.0643 & -0.1137 \end{bmatrix}, \; B_1 = \begin{bmatrix} 580.4780 \\ 65.2800 \end{bmatrix}, \quad C_1 = [0.0198 \;\; 0.9886], \quad D_1 = -0.7304, \tag{27}$$

$-Subsystem - 1.2 - V(26V,\ 1000W)$

$$A_2 = \begin{bmatrix} -0.0958 & -8,4507 \\ 0.0692 & -0.2660 \end{bmatrix}, \; B_2 = \begin{bmatrix} 851.9920 \\ 53.4470 \end{bmatrix}, \quad C_2 = [0.0143 \;\; 0.9886], \quad D_2 = -1.0054, \tag{28}$$

$-Subsystem - 2.1 - V(36V,\ 380W)$

$$A_3 = \begin{bmatrix} -0.3102 & -7.9646 \\ 0.0652 & -0.1119 \end{bmatrix}, \; B_3 = \begin{bmatrix} 542.7340 \\ 68.8140 \end{bmatrix}, \quad C_3 = [0.0199 \;\; 0.9956], \quad D_3 = -0.2802, \tag{29}$$

$-Subsystem - 2.2 - V(26V,\ 380W)$

$$A_4 = \begin{bmatrix} -0.0759 & -8.7329 \\ 0.0715 & -0.0287 \end{bmatrix}, \; B_4 = \begin{bmatrix} 814.2740 \\ 58.5880 \end{bmatrix}, \quad C_4 = [0.0144 \;\; 0.9956], \quad D_4 = -0.3871, \tag{30}$$

where the system are divided in two subsystem in which the polytopes are based in the input voltage and the switching rule follows the output load variation.

Thence, considering $g = 1$, $h = 5$, $R_w = 10I_{1\times1}$ and $\mu = 0.9$, and $u_{max} \leq 0.5$, for time simulation of 300 ms and initial condition $x(0) = [38.5 \; 26]^T$. To switched control law $u(k) = -F_{\sigma(k)} x(k)$, the augmented gain to subsystems are:

$$F_{\sigma(1)} = 1 \times 10^{-3} \, [-0.6575 \;\; 0.7760 \;\; 0.3865] \tag{31}$$

$$F_{\sigma(2)} = 1 \times 10^{-3} \, [-0.6639 \;\; 0.6150 \;\; 0.3978] \tag{32}$$

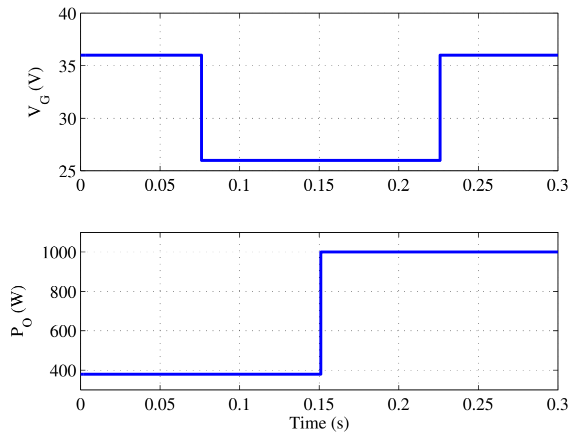

Figura 3. a) Input voltage (V_G)
b) Load Power (P_o).

Figure 3 presents the disturbance variables. The first curve is the input voltage variation V_G displayed in (A) and the second curve is the load power P_o presented in (B). Both curves illustrate the disturbance of boost converter modeled using polytopic uncertainty and switched subsystem.

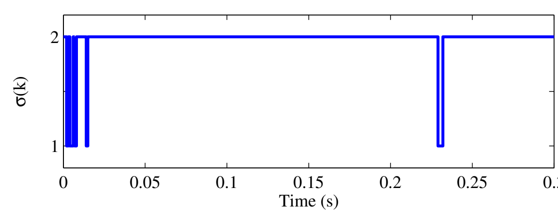

Figura 4. Switching sequence

In Figure 4, it observed that the switching sequence is determined in the simulation as result of switching rule expressed in (13). Besides, Figures 5 and 6 demonstrate the closed-loop stabilization of the proposed SR-MPC strategy. Observing the Figures 3 and 4, the switching chattered more at beginning and stabilized during the rest of simulation, with exception of 2nd input voltage change, in which there was a short variation and stabilized again.

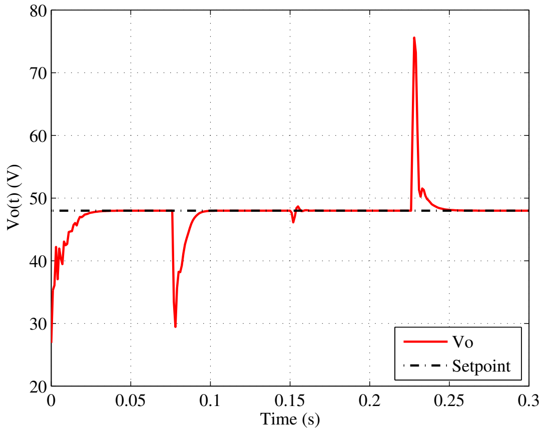

Figura 5. Output voltage (V_o).

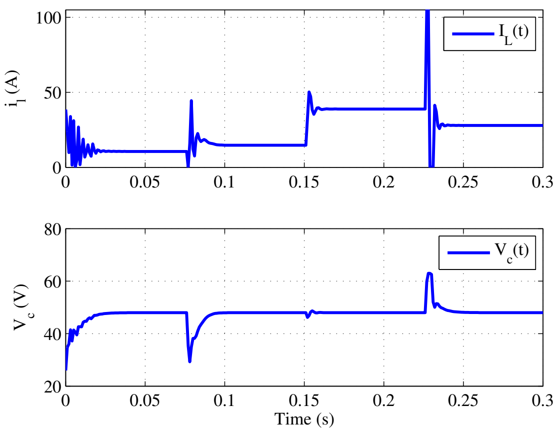

Figura 6. States response

Besides,the Figures 5 and 6 display the time response of inductor current (I_L) and capacitor voltage (V_c). It is observed that the states of boost model are stables in closed-loop and the switching rule keeps its purpose as illustrated in the block diagram of Figure 2. Thus, the proposed control strategy was well succeed to closed-loop stability of the output voltage and the states, maintaining the stability in view of operations changes seen in Figure 3.

Furthermore, the control signal exhibited in Figure 7 demonstrated that the proposed switching design ensured the required specifications considering $u_{max} \leq 0.5$ for nonlinear boost converter model and hold the closed-loop stability in face of changes of operation point presented in Figure 3.

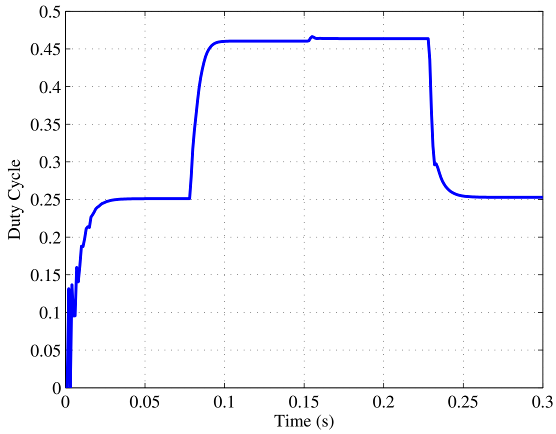

Figura 7. Control Signal.

The boundary ellipsoids for SR-MPC design are presented in Figure 8. Based in Section 3, the boundary ellipsoids aims ensure the closed-loop stability for all the subsystems and are useful for store the obtained stable gains in a lookup-table (Wan and Kothare, 2002). To the boost model,the Figure 8 confirms the stability of the closed-loop model and reinforces that the time response trajectory are inside of ellipsoids for all the states, including the integral action state, where it assures the efficiency and feasibility of the procedure to the boost converter plant.

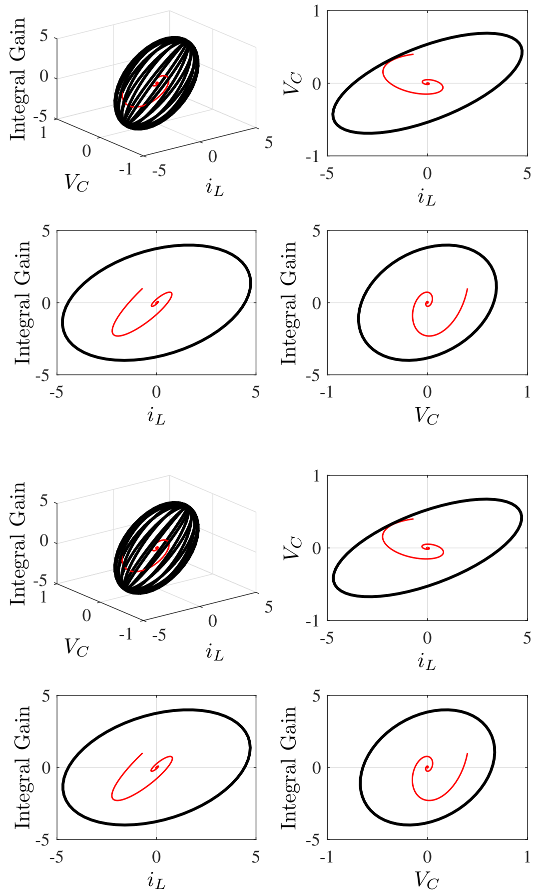

Figura 8. Boundary Ellipsoids.

5. CONCLUSION

This study proposed the switched robust model predictive control applied to voltage control of 3SSC boost converter considering the equivalent boost model. The proposed robust control aimed to ensure the closed-loop output voltage stability of boost converter using the switched rule principle associated with the polytopical uncertainty existent in the presented power converter. Accord to proposed contributions, it is worth to affirm that the SR-MPC-LMI defined in this paper guaranteed the design specifications based of the simulation test adopted in this study. Besides, the presented control technique achieved the feasibility combining polytopical uncertainty and switching rule, overcoming the switched MPC design of Benallouch et al. (2014). Thus, the simulation test analysis demonstrated the efficiency and capability of the SR-MPC-LMI to stabilize the output voltage of 3SSC Boost converter using parameters variation as disturbance of model, being one more alternative control design to DC-DC boost converters. Therefore, the proposed SR-MPC-LMI design based the principle procedure seen in Geromel and Colaneri (2006a); Benallouch et al. (2014) and following offline approaches defined by Wan and Kothare (2002) applied to output voltage stabilization of boost converter was well succeed, confirming the efficiency of this method.

Therefore, the achieved results in this study collaborate to more investigation about switched model predictive control applied to DC-DC converters. As objective to future works is to apply this presented study in an experimental setup aiming to validate the obtained results shown in this paper.

ACKNOWLEDGMENTS

This study was financed in part by the Coordenação de Aperfeiçoamento de Pessoal de Nível Superior - Brasil (CAPES) - Finance Code 001. The authors thank the Universidade Federal do Piauí (UFPI), the Universidade Federal Rural do Semi-Árido (UFERSA) and the Grupo de Estudo em Automação e Controle (GEAC) by the support given to develop this work.

REFERÊNCIAS

Araújo, A.C., Maia, C.V.M.S., and Martins, M. (2019). Controle preditivo com garantia de estabilidade aplicado a um conversor boost. In *Anais do 14º Simpósio Brasileiro de Automação Inteligente*. Galoa. doi:10.17648/sbai-2019-111590. URL https://doi.org/10.17648/sbai-2019-111590.

Bascopé, G. and Barbi, I. (2000). Generation of a family of non-isolated dc-dc pwm converters using new three-state switching cells. *2000 IEEE 31st Annual Power Electronics Specialists Conference. Conference Proceedings (Cat. No.00CH37018)*, 2, 858–863 vol.2.

Benallouch, M., Schutz, G., Fiorelli, D., and Boutayeb, M. (2014). H∞ model predictive control for discrete-time switched linear systems with application to drinking water supply network. *Journal of Process Control*, 24(6), 924–938. doi:10.1016/j.jprocont.2014.04.008.

Cao, B., Grainger, B.M., Wang, X., Zou, Y., Reed, G.F., and Mao, Z.H. (2021). Direct torque model predictive control of a five-phase permanent magnet synchronous motor. *IEEE Transactions on Power Electronics*, 36(2), 2346–2360. doi:10.1109/tpel.2020.3011312. URL https://doi.org/10.1109/tpel.2020.3011312.

Costa, M.V.S., Reis, F.E.U., Campos, J., and Almeida, O.M. (2016). Lpv gain-scheduling control for a phase-shifted pwm full-bridge soft switched converter. *IFAC Proceedings Volumes (IFAC-PapersOnline)*, 19, 6135–6140.

Costa, M., Reis, F., Campos, J., Nogueira, F., and Almeida, O. (2017). Robust mpc-lmi controller applied to three state switching cell boost converter. *Eletrônica de Potência*, 22(1), 81–90. doi:10.18618/rep.2017.1.2652.

Cuzzola, F.A., Geromel, J.C., and Morari, M. (2002). An improved approach for constrained robust model predictive control. *Automatica*, 38(7), 1183–1189. doi:10.1016/s0005-1098(02)00012-2.

Deaecto, G.S. and Geromel, J.C. (2008). Controle de sistemas lineares com comutação. *Sba: Controle & Automação Sociedade Brasileira de Automatica*, 19(4), 431–443. doi:10.1590/s0103-17592008000400006.

Dey, S., Taousser, F.Z., Djemai, M., Defoort, M., and Gennaro, S.D. (2021). Observer based leader–follower bipartite consensus with intermittent failures using lyapunov functions and time scale theory. *IEEE Control Systems Letters*, 5(6), 1904–1909.

Esfahani, P.S. and Pieper, J.K. (2019). Robust model predictive control for switched linear systems. *ISA Transactions*, 89, 1–11. doi:10.1016/j.isatra.2018.12.006.

Fard, H.J. and Sadeghzadeh, S.M. (2021). Predictive control strategy on an the ultra-high gain DC/DC converter suitable for photovoltaic energy conversion system. *Journal of Electrical Engineering*, 72(6), 388–394. doi:10.2478/jee-2021-0055.

Geromel, J.C. and Colaneri, P. (2006a). Stability and stabilization of discrete time switched systems. *International Journal of Control*, 79(7), 719–728. doi:10.1080/00207170600645974.

Geromel, J.C. and Colaneri, P. (2006b). Stability and stabilization of continuous-time switched linear systems. *SIAM Journal on Control and Optimization*, 45(5), 1915–1930. doi:10.1137/050646366.

Hall, R.A. and Bridgeman, L.J. (2021). Computationally tractable stability criteria for exogenously switched model predictive control. *IEEE Control Systems Letters*, 5(5), 1777–1782. doi:10.1109/lcsys.2020.3043866.

Kairuz, R.I.V., Orlov, Y., and Aguilar, L.T. (2021). Prescribed-time stabilization of controllable planar systems using switched state feedback. *IEEE Control Systems Letters*, 5(6), 2048–2053.

Kaitao, B., Lv, H., Chen, L., Li, J., Zhu, Y., Huang, W., and Fan, Q. (2022). A model predictive controlled bidirectional four quadrant flying capacitor dc/dc converter applied in energy storage system. *IEEE Transactions on Power Electronics*.

Khan, S.A., Guo, Y., Khan, M.N.H., Siwakoti, Y., Zhu, J., and Blaabjerg, F. (2020). A novel single source three phase seven-level inverter topology for grid-tied photovoltaic application. In *2020 IEEE 9th International Power Electronics and Motion Control Conference (IPEMC2020-ECCE Asia)*. IEEE.

Kothare, M., , Balakrishnan, V., and Morari, M. (1996). Robust constrained model predictive control using linear matrix inequalities. *Automática*, 32, 1361–1379.

Maestre, J.M., de la Peña, D.M., and Camacho, E.F. (2010). Distributed model predictive control based on a cooperative game. *Optimal Control Applications and Methods*, 32(2), 153–176.

Marcolino, M.H., Galvão, R.K.H., and Kienitz, K.H. (2020). Predictive control of linear systems with switched actuators subject to dwell-time constraints. *Journal of Control, Automation and Electrical Systems*, 32(1), 1–17. doi:10.1007/s40313-020-00667-9.

Middlebrook, R.D. and Cuk, S. (1976). A general unified approach to modelling switching-converter power stages. In *1976 IEEE Power Electronics Specialists Conference*. IEEE. doi:10.1109/pesc.1976.7072895. URL `https://doi.org/10.1109/pesc.1976.7072895`.

Moreira, T., Costa, M., and Nogueira, F. (2021). Output feedback t-s fuzzy rmpc applied to 3ssc boost converter. *Revista IEEE América Latina*, 19, 1520–1527.

Moreira, T., Rego, R., Rios, C., Nogueira, F., and Costa, M. (2019). Análise comparativa entre controlador gpc-t e mpc-lmi com anti-windup lmi aplicado em conversor boost ccte. In *12th Seminar on Power Electronics and Control, At Natal - RN*, 6.

Najson, F. (2021). Spectral and convex uniform exponential stability determination in a class of switched linear systems. *IEEE Control Systems Letters*. doi: 10.23919/acc50511.2021.9483153.

Peccin, V.B., Lima, D.M., Flesch, R.C.C., and Normey-Rico, J.E. (2019). Fast constrained generalized predictive control with admm embedded in na fpga. *IEEE Latin America Transactions*, 18, 422–429.

Rego, R., Moreira, T., Nogueira, F., and Costa, M. (2019). Tube mpc applied to 3ssc boost converter with time-varying parameters disturbance. In *The 12th Seminar on Power Electronics and Control*, 6.

Rego, R.C.B., Costa, M.V.S., Reis, F.E.U., and Bascopé, R.P.T. (2018). Análise e simulação do controlador mpc-aw-lmi aplicado ao conversor ccte operando em condições de saturação no sinal de controle. In *XXII Congresso Brasileiro de Automática*.

Rego, R.C. and Costa, M.V.S. (2019). Controle preditivo baseado em modelo com retroalimentação aplicado no conversor boost com incertezas. In *sbai2019*. Ouro Preto, MG.

Wan, Z. and Kothare, M. (2002). Robust output feedback model predictive control using off-line linear matrix inequalities. *Journal of Process Control*, 12, 763–774.